Polymer 50 (2009) 1197–1205

Contents lists available at ScienceDirect

Polymer

journal homepage: www.elsevier.com/locate/polymer

# High Precision Deposition Electrospinning of nanofibers and nanofiber nonwovens

Ch. Hellmann [a], J. Belardi [a], R. Dersch [a], A. Greiner [a], J.H. Wendorff [a,*], S. Bahnmueller [b,**]

[a] Department of Chemistry and Center of Material Science, Philipps-University, Hans-Meerwein-Strasse, Marburg 35032, Germany
[b] Functional Films Research Center Singapore, Bayer (South East Asia) Pte Ltd, 049514 Singapore, Singapore

ARTICLE INFO

*Article history:*
Received 26 November 2008
Received in revised form
12 January 2009
Accepted 13 January 2009
Available online 20 January 2009

*Keywords:*
Polymer nanofibers
Nonwovens
High Precision Deposition Electrospinning

ABSTRACT

Electrospinning is known to produce nanofiber nonwovens with lateral dimensions in 10 cm up to the meter range meeting thus requirements characteristic of filter, textile or even tissue engineering applications. For particular applications other types of deposition pattern are of benefit (i) in which the deposition area is strongly limited in the lateral dimension, (ii) in which a linear deposition path is oriented along a specified direction or (iii) in which the nonwovens are deposited following a predesigned pattern. This paper reports experimental results for the High Precision Deposition Electrospinning (HPDE) approach introduced by us earlier. It is based on a syringe type die-counter electrode set-up used for conventional continuous electrospinning, the key feature being a reduction of the distance between the spinning die and the substrate from the conventional value of 10–50 cm down to the millimeter and below mm range in order to suppress the onset of bending instabilities and the corresponding spread of the deposition area. The architecture of the nonwovens is controlled in this case by buckling processes and deflections of the jet by transiently charged nanofibers on the substrate. A second important feature of the set-up is a counter electrode/substrate which can be subjected to precise motions in the deposition plane. Based on a careful optimization of the spinning parameters and a tight online control of the spinning process a deposition of individual nanofibers or nonwovens is achieved which meets all deposition requirements specified above. This opens the route towards novel applications among others in areas relying on specific surface architectures such as sensorics, microfluidics and possibly also surfaces of implants.



## 1. Introduction

Electrospinning is known to allow not only the production of planar nonwovens composed of nanofibers from synthetic polymers, polymers of natural origin but also from other classes of materials including metals or ceramics [1–6]. The fiber diameters could be as small as a few nanometer if electrospinning takes place from polymer solutions under appropriate spinning conditions. Such nonwovens meet with strong interest in technical areas – filters, textiles, nanofiber reinforcement – as well as in medicinal areas – tissue engineering, wound healing, drug delivery, etc. [1–6]. For most of these and corresponding applications nonwovens with lateral dimensions in the centimeter up to the meter range are required whereas the thickness may be well down to few micrometers.

In fact, already a conventional laboratory style electrospinning set-up composed of a syringe type die and a planar counter electrode positioned at a distance of the order of 10 cm and above will give rise to the deposition of nonwovens with lateral dimensions of the order of 10–15 cm. The origin of the lateral extension of the deposition area is predominantly the presence of a bending instability characteristic of the electrospinning process [5,7–10]. The jet emanating from the charged droplet at the tip of the die is known to follow a straight path directed towards the counter electrode only for a short distance. It is then subjected to a spiralling looping taking place within a cone shaped envelop having its opening in the direction of the counter electrode. A direct consequence is that the fiber deposition is not strictly localized but happens within an extended deposition area. The same holds for more technically oriented spinning devices composed of a multitude of syringe type dies, of metal spikes arranged along metal wires or along metal cylinders. The spikes assume two roles, they act as solution feeding elements as well as jet initiation elements. The width of the deposition area may be well in the meter range in this case.

* Corresponding author.
** Corresponding author.
*E-mail addresses:* wendorff@staff.uni-marburg.de (J.H. Wendorff), stefan.bahnmueller@bayermaterialscience.com (S. Bahnmueller).

0032-3861/$ – see front matter © 2009 Elsevier Ltd. All rights reserved.
doi:10.1016/j.polymer.2009.01.029

Now for particular applications other types of deposition pattern should be of benefit. It may be required that the deposition path is strongly limited along one of the lateral directions, that it is oriented along a specified direction or that the nonwoven is deposited following a predesigned pattern. Nanofluidics where a guiding pattern composed of hydrophilic or hydrophobic nonwoven might be required on surfaces, microelectronic devices where directed conductive surface structures connecting specific electrode configurations might be the aim or tissue engineering requiring linear fibrillar scaffolds designed to connect cells such as nerve cells are just three examples.

Recently the so-called near field electrospinning was proposed allowing to a certain extent to meet such requirements [11–13]. In one of the proposed approaches a droplet suspended at an AFM tip is subjected to an electric field existing between the tip and a counter electrode which is located at a distance well below the micrometer range [11]. The droplet is deformed by the field and subsequently deposited on a moving substrate in the shape of a rod/short fiber. The scale is in the nanometer range as the droplet diameter is also in the nanometer range. A further approach involves a microfluidic feeding set-up with very fine tips and a rapidly moving take-up substrate [12,13]. A technical realization devoted to larger scale continuous deposition of specific pattern on extended surfaces or to the continuous incorporation of nanofibers/nanorods into particular nanoelectronic devices is not obvious at this stage for these kinds of approaches.

A precision deposition of nanofibers/nonwovens meets in conventional electrospinning with one major problem. The presence of bending instabilities gives rise to looping motions of the jet at the end of a straight path preventing a highly localized deposition. We have recently introduced the High Precision Deposition Electrospinning (HPDE) approach which relies on a conventional die-electrode/counter electrode set-up with continuous pumping of the polymer solution through the die [6,14,15]. The approach is characterized first of all by a very significant reduction of the die/electrode to substrate/counter electrode distance from the conventional several cm- to the mm- and below mm-range. The motivation is that this will give rise to the suppression of the bending instability so that fiber deposition is only controlled by a linear straight jet [5,10–13].

This linear path of the jet will in general only give rise to the deposition of linear nanofibers along the substrate if the deposition speed and the displacement speed of the substrate are very similar i.e. in the range from about 10 cm/s up to several m/s depending on the die/substrate distance [5]. Results for this situation will be reported at first in this paper. Secondly we have chosen the case that the displacement speed is much smaller so that nonwovens are deposited. The expectation is that the localized deposition pattern will in this case be controlled first of all by the onset of buckling processes. Detailed investigations of the buckling phenomenon have revealed a surprising richness of buckling pattern including sinusoidal trajectories, meandering, coiled structures, figure-of-eight structures and many more [16,17]. Buckling is believed to result primarily from the presence of longitudinal compressive forces acting on the impinging thread. The deposition pattern should furthermore become controlled also by deflections of the down-coming jet by the transiently charged nanofibers already deposited highly localized on the substrate. This effect will increase in strength as the speed of fiber deposition increases relative to the displacement speed of the substrate.

The finding to be discussed in some detail in this paper is that one becomes able to deposit individual nanofibers or nonwovens in a highly controlled way both in terms of small fiber diameters and the location and orientation of the deposition. One is even able to "write" specific figures, i.e. pattern by moving the substrates along predetermined paths. The expectation is that these types of precision deposition will give rise to novel applications among others in areas relying on surface properties such as sensorics, microfluidics and possibly also the modification of surfaces of implants.

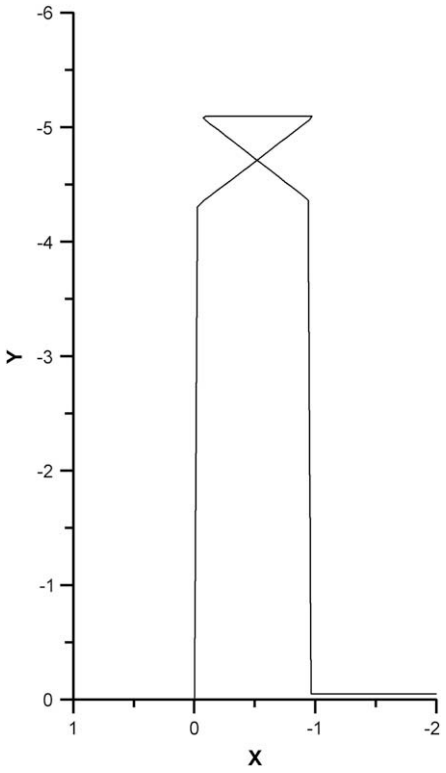


**Fig. 1.** Test pattern devised used to control the deposition of nanofibers by the HPDE approach according to specifications.

## 2. Experimental

### 2.1. Polymer systems

Polymer systems which were electrospun via the High Precision Deposition Electrospinning included first of all polyethylene oxide (PEO) in water. The molecular weight of PEO was chosen to be $9 \times 10^5$ g/mol (Sigma Aldrich), the spinning solutions were characterized by polymer concentrations of 4 w% with a corresponding viscosities of 1.6 Pa s. Such PEO solutions can be spun to nanofibers with conventional electrospinning units giving rise to fiber diameters in the range of 200–1000 nm. Furthermore also solutions with 2 w% PEO were tested, such solutions cannot be spun to fibers free of droplets in conventional set-ups.

In addition polyamide 6 (PA 6, Carl Roth GmbH, unspecified molecular weight) dissolved in formic acid (weight% PA 6 amounting to 15 and 20% yielding fiber diameters in conventional electrospinning from 200 to 1500 nm) were electrospun, the viscosity amounting to 6.7 and 10.7 Pa s respectively. Finally polyacrylonitrile (PAN, Dolan GmbH, molecular weight $8.5 \times 10^4$ g/mol) dissolved in DMF (weight% PAN amounting to 10 and 14% yielding fiber diameters in conventional electrospinning from 400 to 1500 nm) were electrospun by the HPDE approach. The viscosity amounts in this case to 5.7 Pa s for the 14 w% solution.

### 2.2. Precision electrospinning set-up

The High Precision Deposition Electrospinning experiments were performed with an experimental set-up corresponding to

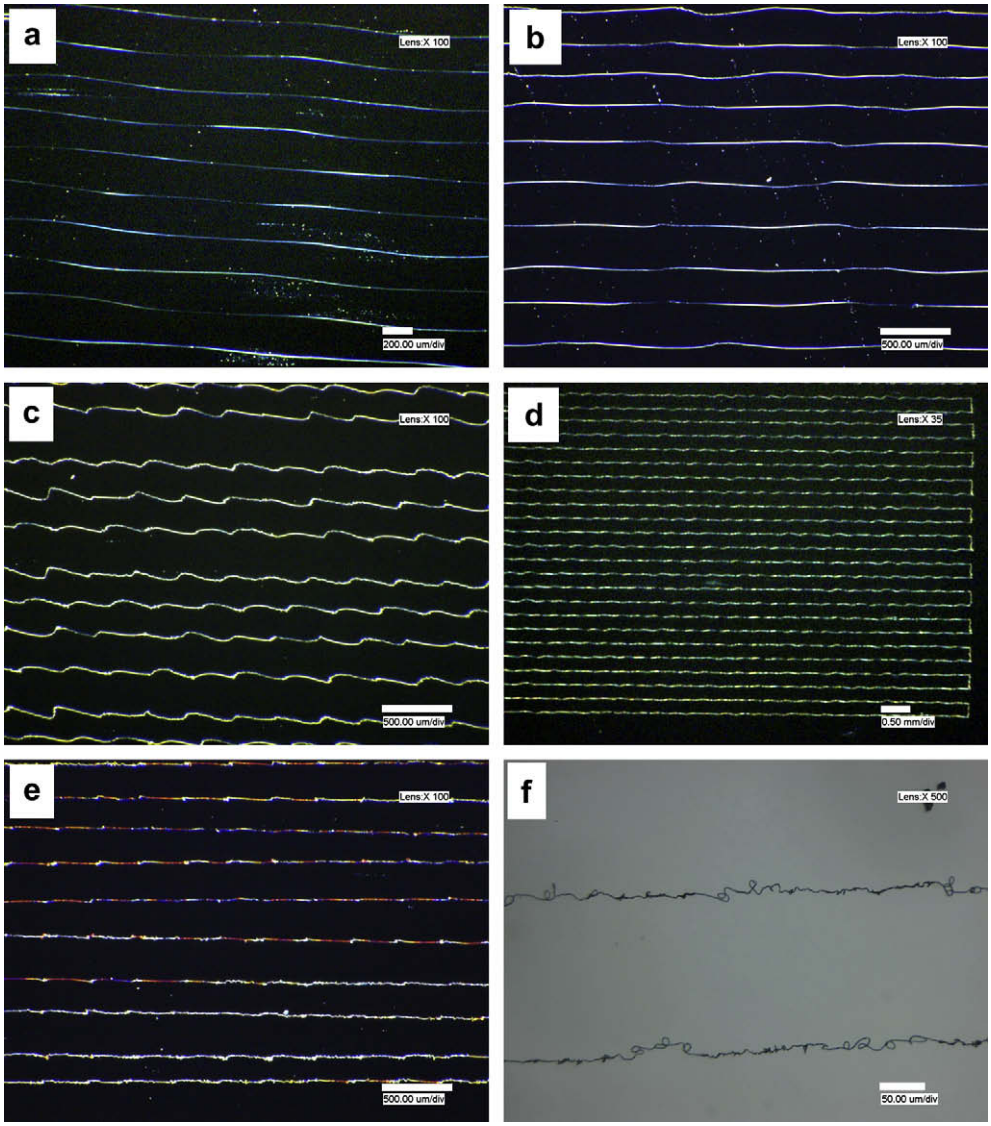


**Fig. 2.** Array of parallel nanofibers composed of PEO (a) and (b) nearly linear trajectories deposited for larger displacement speeds (5 and 3 cm/s), (c) and (d) undulating trajectories for medium displacement speeds (1.9 and 1.4 cm/s) and (e) and (f) buckling trajectories for small displacement speeds (0.75 and 0.47 cm/s).

a conventional laboratory type device. It consist of a high precision pump (Harvard Apparatus, Standard Pump 22 Infusion) which is responsible for a precise feeding rate of the polymer solution through precision bore glass capillaries with accurate dimensions in shape, inner and outer diameter (Hilgenberg GmbH). One modification as compared to the conventional set-up is an inner diameter of the die amounting to 50 μm rather than several 100 μm. These glass capillaries are connected to a high voltage generator (Knürr Heinzinger, PCN-20000-3 ump) via steel adapter and are acting as one electrode. This positive high voltage unit could be controlled externally. A constant negative voltage was applied to a planar counter electrode (Knürr Heinzinger, LNC 20000-3 neg). The applied voltages were in the range from 0.1 to 10 kV.

To induce a continuous spinning process for electrode distances as small as 1 mm and below we monitored the spinning process by optical means using a high resolution camera (Nikon Coolpix 995), additional lenses and a self-made zoom objective.

The planar counter electrode and/or a planar substrate located on top of the counter electrode were mounted on a displacement unit (2 axes micrometer table RK (50/120) Rove Kröger and 1 axis micrometer table ZF1 iselautomation) allowing both horizontal shifts along the *X* and *Y* directions within the plane of the counter electrode as well as vertical displacement causing a modification of the distance between the electrodes. The displacement was controlled via computer allowing thus displacements following a predetermined pattern. The displacement velocity could be varied from 0.1 mm/s up to 8.5 cm/s.

A test pattern was designed (Fig. 1) and the displacement of the substrate was controlled accordingly to find out whether the test pattern can be reproduced via the deposition of nanofibers and nanofiber nonwovens on planar surfaces.

The quantities which were evaluated primarily by optical microscopy were the width of linear deposition lines, the diameter of the fibers resulting from electrospinning as a function of the distance between the electrodes, the applied voltage as well as of the deposition speed. In addition the morphology of the deposited nonwoven was analyzed and the accuracy of the deposition of predetermined pattern was evaluated.

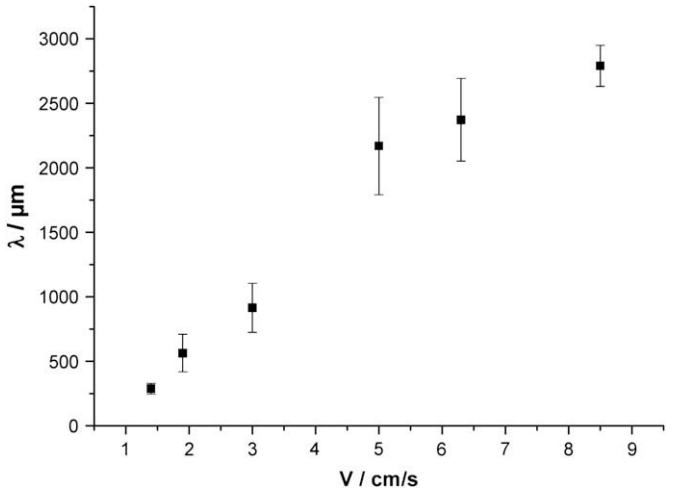


**Fig. 3.** Variation of wavelength of undulations with translational speed of the substrate.

## 3. Results and discussion

### 3.1. Deposition of individual PEO fibers

At first the deposition of individual PEO fibers following a predetermined pattern will be discussed. To write arrays of parallel nanofibers on a silicon wafer the substrate was subjected to rapid displacement along the $+x$-axis followed by an incremental rapid shift along the $y$-axis, a further rapid displacement along the $-x$ direction, etc. The results are shown in Fig. 2a and b for an displacement speed of 5 and 3 cm/s in the $x$-direction. Displacement speed and deposition speed of the fibers were evidently similar in this case.

It is obvious that nearly linear nanofibers are deposited in a regular way parallel to each other. Some slight disturbances were apparent in the paths which resulted from vibrations of the total set-up. To modify the trajectory of the deposited nanofibers towards a periodicity along the fiber axis the displacement speed was reduced. The expectation was that a reduction in the displacement speed along the $x$-direction should result into the formation of undulation to accommodate the increased length of the deposited nanofiber per displacement increment. This effect is apparent in Fig. 2c and d. The change of direction taking place at the end of the linear paths was also geometrically well defined as obvious from Fig. 2d. The undulations became more pronounced i.e. their wavelength got shorter as shown in Fig. 3 as the displacement speed was further reduced.

Finally as the displacement speed was further reduced the fibers started to perform buckling processes to accommodate longer fiber segments per deposition increment (Fig. 2e and f). Buckling is believed to result primarily from the presence of longitudinal compressive forces acting on the impinging jet. Detailed investigations of the buckling phenomenon have revealed a surprising richness of buckling pattern including sinusoidal trajectories, meandering, coiled structures, figures-of-eight structures and many more and the pattern observed here reflect some of the ones reported in the literature [16,17].

The results introduced above demonstrate that electrospinning can be adapted towards writing linear paths with individual nanofibers either with straight shapes or with buckling configurations. The concept is to suppress the onset of the bending motion which would result in strongly looped and thus not precisely localized nanofiber paths. Buckling is the process which defines the architecture of the deposited nanofibers as the displacement speed goes down below a critical value. Of course, one of the problems envisioned to be connected with the suppression of the bending motion is the deposition of fibers with diameters well above the range known for conventional electrospinning that is well in the several micrometer range. The observation, is however, that the fiber diameters obtained for this kind of approach correspond quite well to the ones range known for conventional electrospinning i.e. they are of the order of a few 100 nm for the cases considered here [6,14,15]. One reason certainly is the choice of a very small inner diameter of the die as compared to conventional electrospinning.

The upper speed of depositing nanofibers considered here amounted to the order of 10 cm/s corresponding approximately to the fiber deposition speed. Now, for technical applications much larger speeds may be required. Such speeds can simply be achieved by an increase of the distance between die and substrate as obvious from theoretical calculations [5]. An increase of this distance from 1 mm to 10 mm is predicted to induce a deposition speed of around 3 m/s with the electric field allowing a fine tuning. Fig. 4 compares fiber deposition for the same deposition speed yet for a deposition distance of 1 and 2 mm. The buckling effect becomes more pronounced for the 2 mm distance since the mismatch between deposition and substrate displacement speed increased, the width of the deposition path increased and the deposition pattern approached one of a nonwoven. The deposition of nonwoven paths will be discussed below in more detail.

Similar to linear arrays rectangular arrays of nanofibers oriented both along the $x$ and the $y$ direction could be produced as shown in Fig. 5.

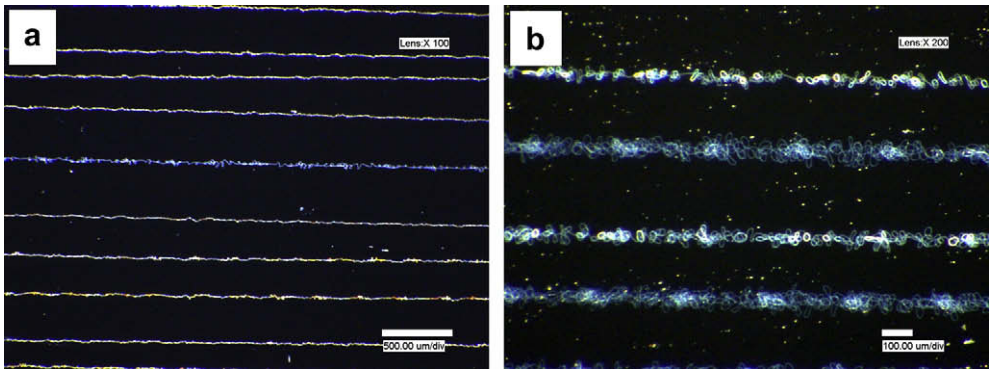


**Fig. 4.** Deposition of nanofibers (speed 0.47 cm/s) with a deposition distance of (a) 1 and (b) 2 mm.

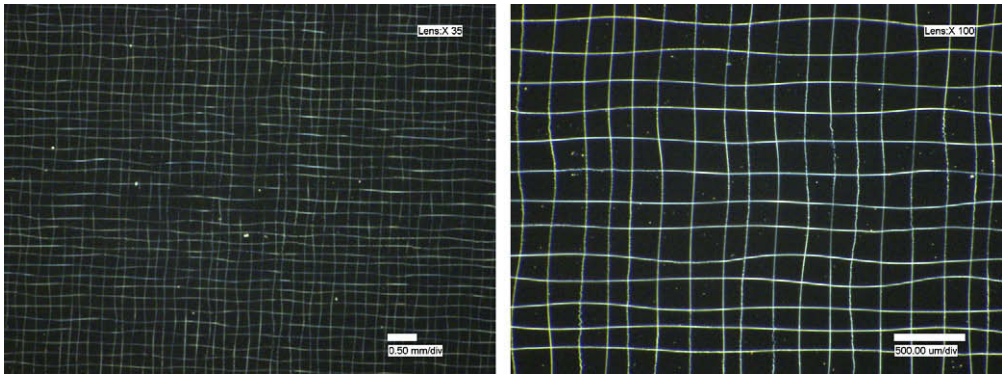


**Fig. 5.** Rectangular arrays of nanofibers (displacement speed = 5 cm/s, distance = 0.5 mm, Voltage = ~1 kV).

Some crosstalk originating from the interaction between the charged fibers crossing each other caused some disturbances of the regularity of the array across the total pattern. The total width of the pattern corresponded in the cases considered here to be $25 \times 25\ cm^2$.

### 3.2. Deposition of PEO nanofiber nonwovens paths

The main topics of interest to be discussed as far as precision electrospinning of nonwoven paths is concerned are (i) the control of the width of the deposition area of the nanofiber nonwovens among others by the electrode distances, the applied voltage and the displacement velocity, (ii) the architecture of the nonwoven deposited as well as the fiber diameter of which the nonwoven is composed and finally, (iii) the deposition of well defined nonwoven pattern in terms of their exact location, orientation and shape. Results on these topics will be discussed in the following concentrating at first on spinning solutions composed of PEO and water. We will subsequently also discuss results obtained for PA 6/formic acid spinning solutions and PAN/DMF spinning solutions which are frequently also used in conventional electrospinning. It has to be pointed out at the beginning that the determination of the width of the area onto which fibers are deposited is done in general for a substrate/counter electrode which is displaced horizontally relative to the fixed die with a given displacement velocity. The extrapolation to a nonmoving substrate as used in conventional electrospinning will be considered below for specific cases.

Theoretical treatments and experimental observations related to buckling phenomena and jet deflection discussed above suggest that the distance between the die acting as one electrode in electrospinning and the counter electrode/substrate should be one of the principle parameter controlling the deposition area. Fig. 6a–c displays optical images of the result of deposition experiments for PEO/water spinning solutions for electrode distances ranging from

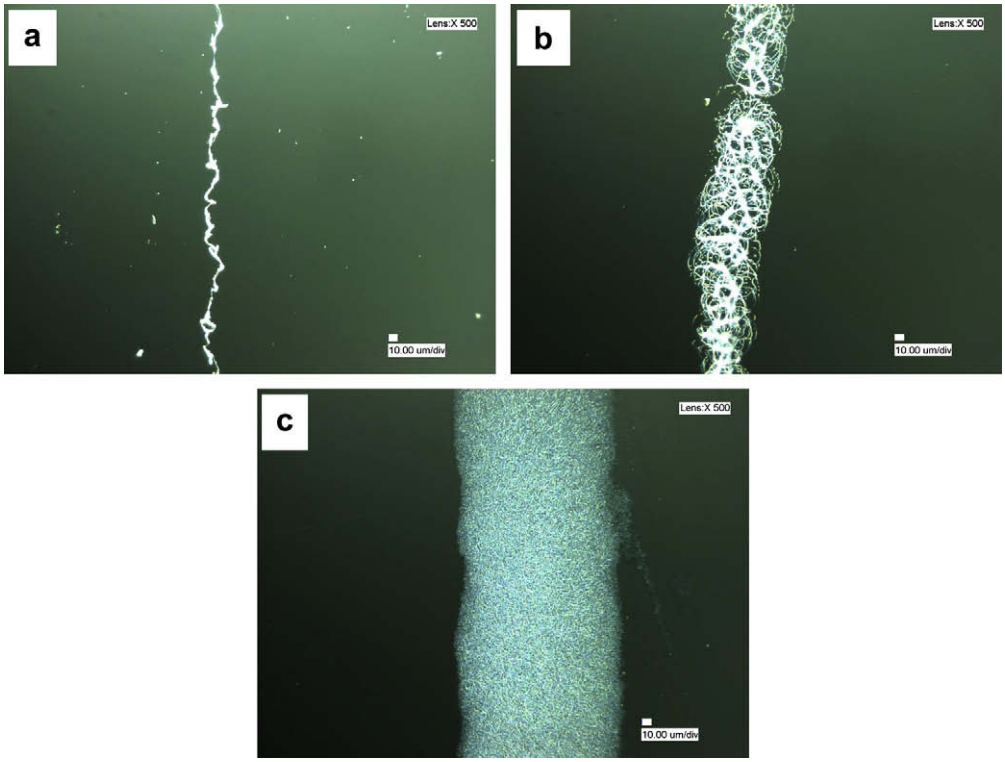


**Fig. 6.** Path of PEO fibers from 4 w% PEO/water solutions for different electrode distances obtained via a linear motion (1 mm/s) of the counter electrode relative to the die as a function of the electrode distance: (a) 0.5 mm, (b) 2.5 mm, (c) 10 mm, applied voltage 2 kV in all cases.

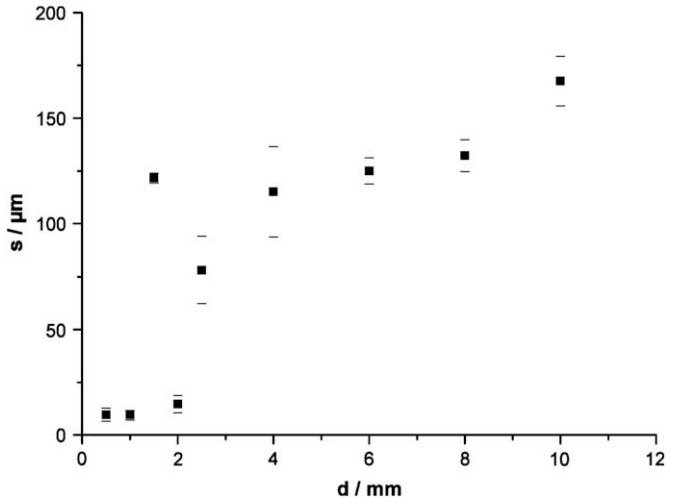


**Fig. 7.** Dependence of the width of the deposition path on the electrode distance for a solution of 4 w% PEO in water (Applied voltage 4 kV, displacement velocity of the counter electrode 1 mm/s).

0.5 mm up to about 10 mm. All experiments were performed using a linear displacement of the substrate with a displacement velocity of 1 mm/s and an applied voltage of 2 kV. It is apparent that fibers were deposited in all cases and that the linear displacement of the substrate caused the deposition of a linear path composed of these fibers.

An electrode distance of about 0.5 mm led to a roughly linear deposition of fibers which showed buckling features with the path width amounting to just a few micrometers. An increase of the electrode distance to about 2.5 mm resulted in a corresponding increase of the width of the linear structure, the deposition density is enhanced, individual fibers with loops as expected from buckling effects could still be observed. The width of the linear path now amounts to about 10 µm. Finally the width of the path amounts to about 40 µm for the largest electrode distance tested here (10 mm) and the arrangement of the fibers within this linear structure resembled one of nonwovens obtained by conventional electrospinning i.e. a dense deposition of planar randomly oriented nanofibers has taken place. These results already showed without any doubt that continuous electrospinning can be performed to produce nonwovens with electrode distances down to the micrometer range and below and that one is able to deposit specific very narrow deposition pattern as controlled by the motion of the counter electrode. In the following the parameters which control the deposition width, the fiber arrangement as well as the fiber diameter will be analyzed in a quantitative way.

Fig. 7 displays the variation of the width of the linear deposition path in absolute numbers as the electrode distance is varied from 0.5 mm to about 10 mm. The observation is that the width of the deposition path is increased in this case from about 10 µm up to about 170 µm and above (see Fig. 6c) i.e. one is able to obtain a controlled localization of the deposition area via the choice of the electrode distances.

The variation of the deposition width with electrode distance does not seem to be linear but rather increased for intermediate distances in a weakly stepwise manner. To interpret this finding one has to keep in mind that the deposition speed increases strongly with increasing electrode distance and decreasing voltage [5] typically from some 10 cm/s to several m/s as the distance is increased from 1 mm up to 10 mm [5]. This causes, as already apparent from Fig. 2, an enhancement of buckling processes with a corresponding increase in the width of the deposition path. It seems, in addition, very well possible that a transient charge is built up at the deposition site due to the rapid localized fiber deposition. This may induce a charge controlled deflection of the incoming jet causing a further spread of the deposition path superimposed on the buckling effect.

An extrapolation to an electrode distance of the order of 10 cm, as used in conventional syringe type set-up, yielded a deposition width of about 2 mm which is well below the actually observed one. This is not surprising in view of the fact that the deposition is controlled by the onset of the bending instability for larger electrode distances which is neglected in the extrapolation.

It seems feasible in view of the nature of the buckling and charge deflection effects that the path width will depend also on the velocity of the counter electrode/substrate [14,15]. The corresponding results are shown in Fig. 8a. The observation is that the width can be strongly reduced with increasing displacement velocity, for instance, down from about 60 to 20 µm for a given set of applied voltage and electrode distance. This dependence is nicely illustrated in Fig. 8b in which spinning was performed at first without displacement of the counter electrode – giving rise to a circular deposition pattern – followed by a linear displacement yielding a deposition path with a width which is smaller by a factor of about 8 in comparison to the diameter of the circular deposition pattern. An increase in displacement velocity will decrease both buckling as well as charge deflection contributions towards path width.

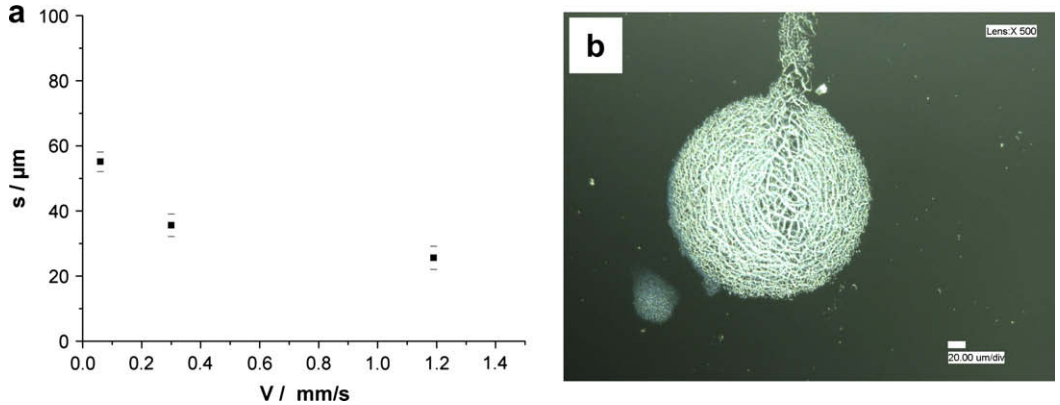


**Fig. 8.** a) Dependence of the width of the deposition path on the displacement velocity of the counter electrode ($d = 1$ mm, 1.85 kV). (b) Deposition with and without displacement of the counter electrode, for 4 w% PEO in water (2 kV).

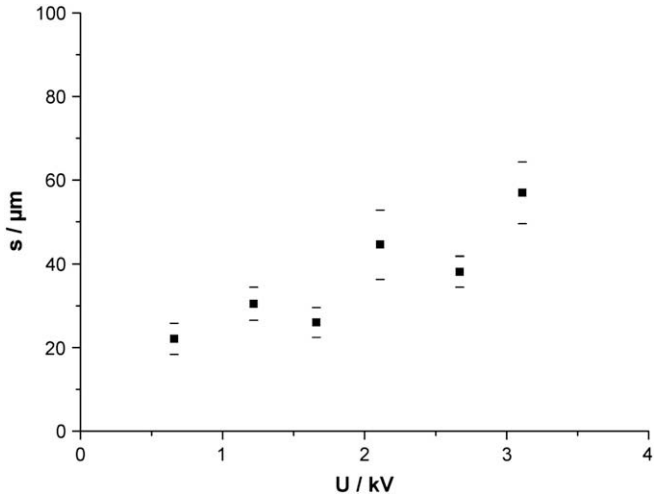


**Fig. 9.** Effect of the applied voltage on the width of the deposition path at constant electrode distance of 1 mm and of a displacement velocity of 1 mm/s.

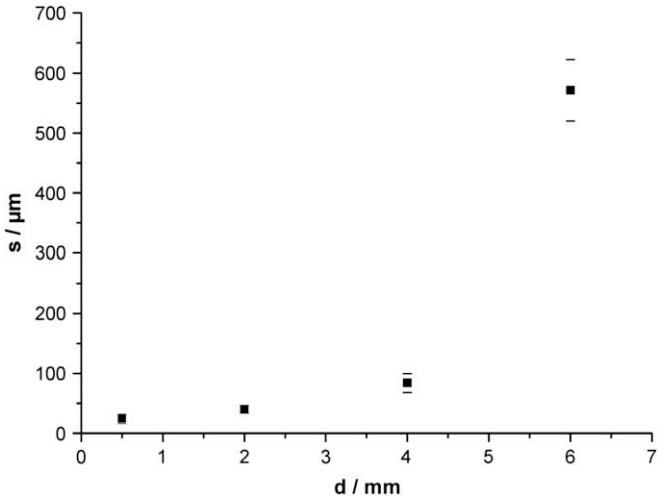


**Fig. 11.** Deposition of PAN fibers from PAN/DMF solutions: dependence of path width on electrode distances (2 kV).

Fig. 9 reveals that for a given value of the electrode distance one may furthermore vary the width of the deposition path via the applied voltage. One effect of an increased voltage is that it tends to draw more fluid from the solution reservoir and to decrease the velocity of the deposition [5]. Both effects would cause the path diameter to shrink. On the other hand the deflection effect induced by the transiently charged fibers may increase in strength since the fibers carry a larger charge density. In any case an increase of the voltage from about 0.5 to 4 kV gives rise to an increase of the width of the deposition path from about 20 to about 60 µm at an electrode distance of 1 mm. Here the increase seems to be roughly linear with increasing voltage.

The optical images of the deposition path displayed above (Figs. 6 and 8) reveal that nanofibers are deposited and that the arrangement of the fibers tend to be isotropic as controlled by buckling/deflection processes: loops and helical structures are among the deposition features. This is obvious, for instance, from Fig. 6a and b. The fibers were randomly oriented within the plane of deposition. A further decrease of the electrode distance and the corresponding strong decrease in deposition speed [5] gave rise to a looped fiber arrangement in the deposition path with the loop density decreasing with further decrease of the electrode distance until single fiber deposition may occur (Fig. 2).

With respect to the diameters of the deposited fibers one has to take into account the fact that the elongational deformation happening in the linear path of the jet is limited assuming values of the order of up to 1000 as compared to the total elongational deformation of a jet subjected to the bending instability of typically 40 000 [5]. The deposited fibers might therefore be expected to display larger fiber diameters and furthermore to be still wet so that they subsequently merge to films or decompose via Rayleigh instabilities to droplets [6].

Actually the nanofibers which are deposited in the HPDE approach do not show any tendency towards Rayleigh instabilities and have diameters which are not too different from the ones obtained for the same spinning solutions in conventional set-ups involving electrode distances of 10 cm and above. The diameters amount in the HPDE approach described here to about 400 nm for larger electrode distances but they may well be in the above 1000 nm range for smaller electrode distances (Fig. 10). Actually very recently a paper was published on the so called continuous near-field electrospinning (although no real near field effects were

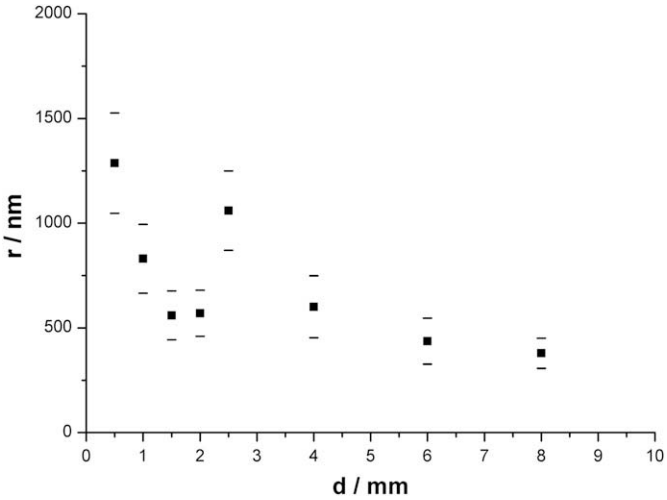


**Fig. 10.** Variation of the fiber diameter with the electrode distance for 4 w% PEO in water (2 kV).

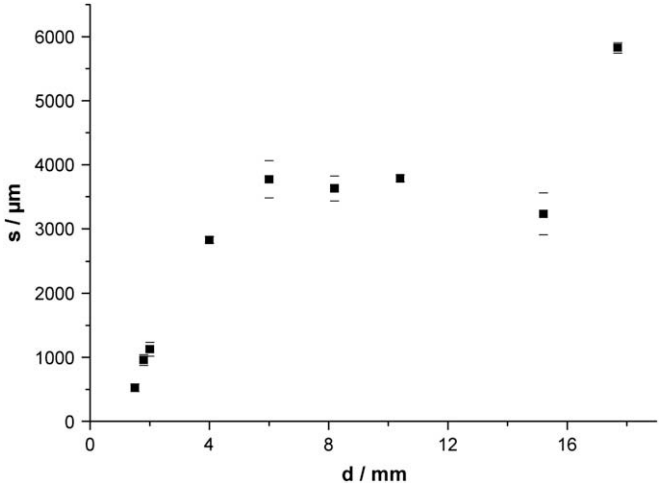


**Fig. 12.** Dependence of path width on electrode distances for PA6 spun from formic acid solution (2 kV).

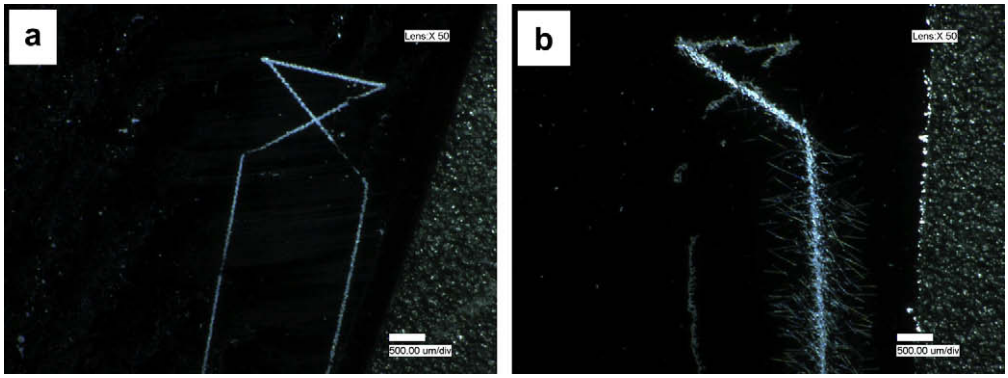


**Fig. 13.** Deposition of test pattern from PAN/DMF solution for electrode distances of 2 and 4 mm (2 kV).

demonstrated) for the deposition of orderly patterns which used the high precision deposition approach introduced by us earlier [6,14,15] for water PEO solutions, electrode distances between about 0.5 mm and 1.5 mm and which reported fiber diameters between about 40 and 2300 nm depending on the applied voltage and polymer concentration [18].

### 3.3. Electrospinning of PAN/DMF solutions

The experimental results obtained for electrospinning of PAN/DMF solutions correspond qualitatively to the ones reported above for the electrospinning of PEO/water solutions. High Precision Deposition Electrospinning gives rise to the deposition of nonwovens composed of nanofibers within a very narrow linear deposition path for the case that the counter electrode/substrate is displaced accordingly. The path width is found to depend strongly on the counter electrode distance and to a certain extent also on the applied voltage at constant electrode distance and on the displacement velocity. The width of the deposition path is found to be as small as about 20 μm for an electrode distance of 0.5 mm and it increased to about 600 μm as the electrode distance increased to 6 mm (Fig. 11). This increase is much stronger than experienced for the PEO/water solution possibly to stronger transient charges located on the deposited fibers.

The applied voltage is found to increase the path width quite significantly similar to the case of the PEO system. The path width can be increased, for instance, from about 25 to 250 μm as the voltage is increased from 2 to 6 kV. The fiber diameter turned out to be of the order of 750 nm and to be rather insensitive to the electrode distance and the applied voltage.

### 3.4. Spinning of PA 6/formic acid solutions

Polyamid 6/formic acid solutions electrospun with the High Precision Deposition set-up yielded nanofibers with diameters in the range of about 500 nm, quite similar to the case of spinning of the PEO and PAN solutions. This diameter range furthermore corresponds to the one found also for conventional electrospinning approaches. Yet the deposition path is much broader then experienced for the other polymer solutions. It amounted to about 500 μm for the shortest electrode distance of 0.5 mm and it goes up to 6000 μm for an electrode distance of 16 mm (Fig. 12).

### 3.5. Deposition of nonwoven test pattern

A major goal of developing the High Precision Deposition Electrospinning was to enable to deposit well defined pattern composed of nonwovens on specific surfaces. The experimental finding is that the deposition of fibers via the HPDE approach does not only yield linear deposition paths but can be strictly controlled by the motion of the counter electrode to result predetermined pattern. Fig. 13 shows that the test pattern introduced in the experimental part can be reproduced in terms of a nonwoven path by the HPDE approach for sufficiently small electrode distances. The diameter of the path of which the pattern is composed can be as small as 20 μm and below. Spinning from PAN/DMF solutions were taken as an example here yet very similar results can be obtained for PEO. It is obvious that the resolution of the deposited pattern decreased with increasing electrode distance due to an increase of the path width discussed above. This is also illustrated in Fig. 13b.

From the results reported above it is obvious that the resolution of the pattern deposition can furthermore be controlled via the

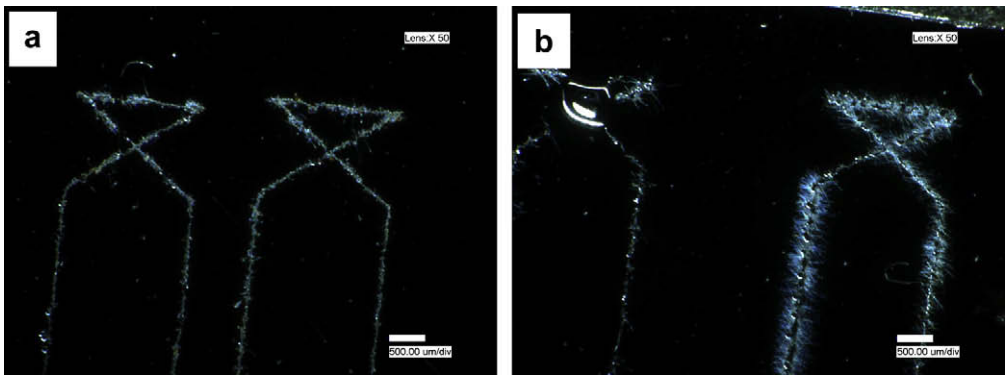


**Fig. 14.** Variation of the pattern resolution with increasing voltage at constant electrode distance of 2 mm (a) 3 kV, (b) 6 kV.

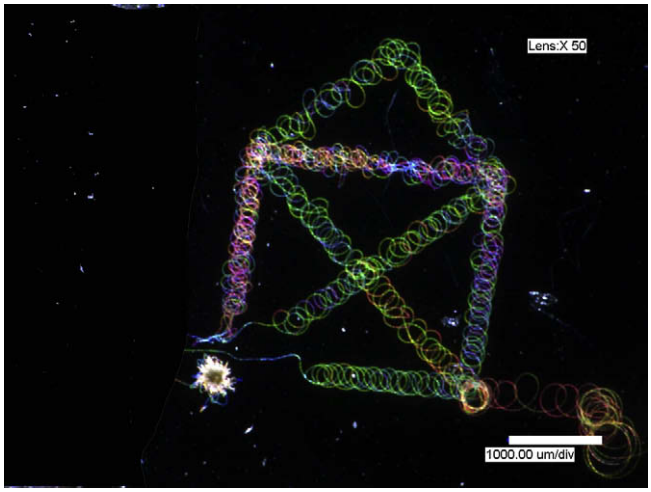


**Fig. 15.** "House of Santa Claus" motif written by PAN nanofibers (distance = 2.2 mm, Voltage = 0.47 kV).

displacement velocity and the applied voltage at constant electrode distance. Fig. 14 represents as an example the variation of the pattern resolution with an increase of the applied voltage obviously being induced primarily by deflection processes.

Electrospinning of PA 6 from formic acid solutions yielded, as described above, very broad deposition paths even for small electrode distances. So pattern resolutions below about 500 μm does not seem to be possible so that only larger pattern can be reproduced with PA 6 fibers.

By displacing the substrate following a predetermined pattern, the pattern can be reproduced via the deposition of nanofibers on a given substrate. Using polyacrylonitrile dissolved in DMF as a further model system the "House of Santa Claus" pattern has been written on a silicon surface (Fig. 15). The deposition pattern being characterized by small loops known to originate from buckling processes. The colors are due to interference effects.

This shows, fiber arrangements following different trajectories can be written on the surface of a given substrate in a well defined way.

## 4. Conclusions

This paper considers results obtained for the High Precision Deposition Electrospinning (HPDE) approach based on the experimental die-counter electrode set-up used for conventional continuous electrospinning in which the distance between the two electrodes is reduced from the usual 10–20 cm down to the millimeter range and below. It is shown that it is possible to strongly limit the width of the deposition area in the lateral dimension in a controlled way, to achieve a linear deposition path which is oriented along a specified direction and to prepare nonwovens following a predesigned pattern. The die/substrate distance, the applied voltage and also the displacement velocity can be used to fine-tune the deposition. The nonwovens are composed in all cases of fibers with diameters in the several 100 nm range, the diameter resembling those obtained for similar polymer solutions using conventional electrospinning set-ups.

The actual width of the deposition path turns out to depend at constant spinning parameters strongly on the polymer system. Polyamide 6 yields path widths which are by more than a factor of 10 larger than the ones found for polyethylene oxide or polyacrylonitrile. PAN turns out to be more sensitive with respect to an increase of the electrode distance than PEO. The sensitivity towards buckling effects and charge deflection effects seem to depend on the combination of polymer and solvent chosen for electrospinning. The important conclusions are that the concept of High Precision Deposition Electrospinning works well for the deposition of individual nanofibers and nanofiber nonwovens following specific pattern. Therefore, opens thus the route towards novel applications among others in areas relying on specific surface architectures such as sensorics, microfluidics and possibly also for the modification of surfaces of implants.

## Acknowledgement

We gratefully acknowledge the financial support by the Bayer MaterialScience AG (Germany). The electronic and mechanic workshop of the Philipps-Univeristät Marburg were extremely helpful in the construction of the electrospinning set-up.

## References

[1] Huang ZM, Zhang YZ, Kotaki M, Ramakrishna S. Compos Sci Technol 2003;63:2223.
[2] Dersch R, Greiner A, Wendorff JH. Dekker encyclopedia of nanoscience and nanotechnology. In: Schwartz JA, Contesen CJ, Putger K, editors. New York: Marcel Dekker; 2004. p. 2931.
[3] Li D, Xia Y. Adv Mater 2004;16:1151.
[4] Greiner A, Wendorff JH. Angew Chem Int Ed 2007;119:5750.
[5] Reneker DH, Yarin AL, Zussman E, Xu H. Adv Appl Mech 2007;41:44.
[6] Greiner A, Wendorff JH. Adv Polym Sci 2008;219:207–71.
[7] Reneker DH, Yarin AL, Fong H, Koombhongse S. J Appl Phys 2000;87:4531.
[8] Yarin AL, Koombhongse S, Reneker DH. J Appl Phys 2001;90:4836.
[9] Hohman MM, Shin M, Rutledge G, Brenner MP. Phys Fluids 2001;13:2201.
[10] Hohman MM, Shin M, Rutledge G, Brenner MP. Phys Fluids 2001;13:2221.
[11] Li D, Wang Y, Xia Y. Nano Lett 2003;3:1167.
[12] Kameoka J, Craighead HG. Appl Phys Lett 2003;83:371.
[13] Kameoka J, Orth R, Yang Y, Czaplewski D, Mathers R, Coates GW, et al. Nanotechnology 2003;14:1124.
[14] Belardi J. Diploma thesis, Marburg; 2007.
[15] Dersch R, Graeser M, Greiner A, Wendorff JH. Aust Chem J 2007;60:719–28.
[16] Chiu-Webster S, Lister JR. J Fluid Mech 2006;569:89–111.
[17] Han T, Reneker DH, Yarin AL. Polymer 2007;48:6064–76.
[18] Chang CH, Limkrailassiri K, Lin L. Appl Phys Lett 2008;93:123111.